Pergamon

Int. J. Heat Mass Transfer. Vol. 38, No. 12, pp. 2239–2250, 1995

0017-9310/95 $9.50 + 0.00

0017-9310(94)00351-3

Numerical simulation of the fluid flow and the mixing process in a static mixer

E. LANG and P. DRTINA
Fluid Dynamics Laboratory, Sulzer Innotec AG, 8401 Winterthur, Switzerland

and

F. STREIFF and M. FLEISCHLI
Sulzer Chemtech AG, 8404 Winterthur, Switzerland

(*Received* 4 *October* 1993 *and in final form* 17 *October* 1994)

Abstract—The fluid flow and the mixing process in a static mixer have been analysed to gain insight into the character of the mixing process and to check the numerical simulation as a tool for the design of single mixers and entire facilities with mixers incorporated. In a first step the mixing process in a straight pipe has been analysed by a numerical simulation, and good agreement has been found with experimental data. The investigation has been extended to an infinite, ideal mixer element. The vortices generated by the structure of the mixer have been observed to be the main driving force of the mixing of the fluid. This is the reason why the main mixing occurs in the wake of the mixer. As an industrial application the fluid flow and the mixing in the inlet part of a denitrification facility has been computed. It has been found that mixing quality is improved significantly by incorporating a static mixer. The measured velocity and concentration data also agree well with the numerically obtained results.

1. INTRODUCTION

The mixing of fluids of differing composition or temperature is a common operation in process industry. The fluids are mixed to get homogeneous distributions of the fluid properties, as this is essential for various chemical processes. Mixing by natural turbulent diffusion is not very efficient. A pipe of a length of 100–200 diameters would be needed to get a well mixed fluid, and this is not practicable. Because of this, static mixers are used to achieve the mixing efficiently in short distance with small pressure losses.

There are various static mixing devices in use to obtain a mixed fluid with minimal pressure drop. The devices usually guide some part of the fluid flow across the pipe or channel to achieve a homogenisation of certain fluid properties. A short overview of various static mixer types is given by Godfrey [1].

Tauscher *et al.* [2] investigated experimentally the performance of the SMV mixer for various industrial applications. Zogg [3] studied the mixing quality and the fluid behaviour under laminar flow conditions in a Sulzer mixing element in his Ph.D. thesis. Gaiser [4] characterised the different flow patterns in stacked corrugated sheets which are geometrically similar to the Sulzer SMV mixer structure (under investigation in this article), and measured the mass transfer coefficient for several parameters. The research of Zogg and Gaiser was mostly experimental, of a more basic character, and limited to the flow field within the static mixer. In this work the fluid flow and the mixing process are investigated for conditions more relevant to industrial applications.

An important application of static mixers is their use in denitrification ($DeNO_X$) facilities. To date, the design of a $DeNO_X$ facility has been optimized and checked by a series of experiments. A scale model is built, and tests are carried out at the same velocity as in reality. Profiles of velocity, temperature and concentration are measured in certain predefined cross sections. Numerical simulation of these facilities has the advantage that data for the whole flow field is obtained. This information serves to optimize and check the design more easily and in a more cost effective manner, see Drtina *et al.* [5].

The aim of this work was twofold: firstly to analyse and understand the mixing process in the static mixer SMV, and secondly to check the ability of numerical simulation as a tool for the basic design and development process of static mixers and of facilities with mixers incorporated.

In the following section the governing equations are described. In Section 3 numerically obtained results of the mixing process in a straight pipe are compared to measured data to check the validity of the computation. That section is followed by an investigation of the mixing process in the static mixer SMV. The underlying flow structure and the mixing process are described. In the fifth section the computation of the fluid flow and the mixing process in an industrial application, a $DeNO_X$ facility, is reported.

NOMENCLATURE

B	width
c	species concentration
c_p	specific heat at constant pressure
D	mass transfer coefficient
d	diameter
d_h	characteristic length
H	height
h	enthalpy
I	turbulence intensity
k	turbulent kinetic energy
$\mathbf{j}$	mass flux
L	length
L_t	turbulent length scale
P	pressure
q	heat flux
R	mass source or sink
Re	Reynolds number
T	temperature
t	time
U_i	mean velocity component
u_i	velocity component
u_i'	fluctuating part of the velocity component
u, v, w	velocity components
x, y, z	Cartesian coordinates.

Greek symbols

ε	dissipation rate
λ	thermal conductivity
μ	dynamic viscosity
ρ	density
σ	intensity of segregation
τ	shear stress.

Subscript

l	left
m	middle
r	right
M	mixer.

Superscript

$\bar{}$	averaged quantities.

2. THE GOVERNING EQUATIONS

The equations for conservation of mass, momentum and species concentration must be solved to calculate the mixing process in a static mixer element. We consider the fluid as being incompressible and stationary. The equations to solve are

$$\frac{\partial}{\partial x_j}(u_j) = 0 \tag{1}$$

for mass conservation,

$$\rho \frac{\partial}{\partial x_j}(u_j u_i) = -\frac{\partial P}{\partial x_i} - \frac{\partial \tau_{ij}}{\partial x_j} + S_{ui} \tag{2}$$

for momentum conservation and

$$\frac{\partial}{\partial x_j}(u_j c) = \frac{\partial \mathbf{j}_j}{\partial x_j} + S_c \tag{3}$$

for species concentration. The molecular fluxes τ_{ij} and $\mathbf{j}_j$ are expressed in terms of velocities and concentration gradients using Stokes' and Fick's laws

$$\tau_{ij} = -\mu\left(\frac{\partial u_i}{\partial x_j} + \frac{\partial u_j}{\partial x_i}\right) + \tfrac{2}{3}\mu \frac{\partial u_k}{\partial x_k}\delta_{ij} \quad \text{and} \tag{4}$$

$$\mathbf{j}_j = -D\frac{\partial c}{\partial x_j}. \tag{5}$$

The program TASCflow of *A*dvanced *S*cientific *C*omputing Ltd. was used to compute the fluid properties. To study the mixing process the flow region of interest had to be split into several subregions in the main flow direction. This reduced the requirements for computer memory and gave reasonable computing times. We assumed that the flow in a downstream subregion does not affect the flow behaviour in the upstream subregion, or respectively that the effects are negligible. This required that profiles of the fluid properties at the outlet of a subregion could be written to a file and be read in as inlet boundary conditions of the next subregion. In the current version of TASCflow this was only possible for velocity components, turbulence properties and temperature but not for concentration. Thus we used the energy equation and computed the temperature distribution instead of computing the concentration. The equation for the concentration of a species

$$u\frac{\partial c}{\partial x} + v\frac{\partial c}{\partial y} + w\frac{\partial c}{\partial z} = D\nabla^2 c + R \tag{6}$$

has a similar form as the energy equation

$$u\frac{\partial T}{\partial x} + v\frac{\partial T}{\partial y} + w\frac{\partial T}{\partial z} = \frac{\lambda}{\rho c_p}\nabla^2 T + \frac{\mu}{\rho c_p}\left(2\left[\left(\frac{\partial u}{\partial x}\right)^2 + \left(\frac{\partial v}{\partial y}\right)^2 + \left(\frac{\partial w}{\partial z}\right)^2\right] + \left(\frac{\partial u}{\partial y} + \frac{\partial v}{\partial x}\right)^2 + \left(\frac{\partial u}{\partial z} + \frac{\partial w}{\partial x}\right)^2 + \left(\frac{\partial v}{\partial z} + \frac{\partial w}{\partial y}\right)^2\right)$$

see Bird *et al.* [6]. As there are no sources in our case, the source term in the concentration equation can be omitted. The factor $\mu/\rho c_p$ in the energy equation is very small of the order of $O(10^{-5})$, hence all the terms multiplied by that factor are negligible. Thus both equations are of the same character. The energy equation can therefore be used instead of the concentration

equation to calculate the mixing process, if the thermal conductivity is calculated to be

$$\lambda = D\rho c_p. \tag{7}$$

In our case the flow in the SMV mixer is turbulent. Due to the enormous range of length and time scales the above mentioned equations cannot be solved numerically by resolving the complete spatial and transient behaviour at high Reynolds number flow. The equations are therefore converted to a mean form, by a time averaging process. Each dependent variable is decomposed into a mean and fluctuating component

$$u_i = U_i + u_i'. \tag{8}$$

With this substitution, the equations reduce to the following form

$$\frac{\partial(\rho U_j)}{\partial x_j} = 0 \tag{9}$$

for the continuity equation,

$$\frac{\partial(\rho U_j U_i)}{\partial x_j} = -\frac{\partial P}{\partial x_i} - \frac{\partial}{\partial x_i}(\overline{\tau_{ji}} + \rho\overline{u_i' u_j'}) \tag{10}$$

for the momentum equation and

$$\frac{\partial(\rho U_j h)}{\partial x_j} = -\frac{\partial}{\partial x_i}(q_j + \rho\overline{h' u_j'}) \tag{11}$$

for the energy equation. Equations (10) and (11) contain terms that are not expressible in terms of mean flow variables. The well known $k-\varepsilon$ model is used to evaluate the Reynolds stress terms $\overline{\tau_{ji}}$, $-\rho\overline{u_i u_j}$ and the turbulent heat transfer terms $\rho\overline{h' u_j'}$ (see Launder and Spalding [7]).

The computer program calculates the continuity, the momentum and the energy equations by applying a finite volume scheme. A general description of the procedure used by TASCflow to solve these equations can be found in the TASCflow user manual [8].

3. THE MIXING PROCESS IN A STRAIGHT PIPE

Hartung and Hiby [9] performed an experiment where two fluid flows, one with sulphuric acid of a certain concentration and the other with caustic soda of a certain concentration, were mixed in a straight pipe. They evaluated the intensity of segregation

$$s = \frac{\sigma^2}{\sigma_0^2} \tag{12}$$

along the pipe by an optical measurement technique. The variation σ is defined as

$$\sigma = \frac{\sum_{i=1}^{n} (C_i - \bar{C})}{n-1} \tag{13}$$

where σ_0 denotes the standard deviation at the inlet, and n is the number of sample points in a cross section of the pipe. In our case it is equivalent to the number of grid points in a cross section.

At the inlet the pipe is split into two semi circle cross sections by a splitter plate. The diameter of the pipe was $d = 0.019$ m, the length $L = 120 \cdot d$. The length of the splitter plate was $L_{sp} = 20 \cdot d$. The inlet velocity of the two fluids was $v = 0.42$ m s^{-1} which yields a Reynolds number of $Re = 8000$. The mixing process in this experiment is entirely driven by turbulent diffusion. This experiment was used to check the results of our numerical simulation.

3.1. *Grid and boundary conditions*

A grid of the pipe was generated which resolves the pipe including the splitter plate at the inlet. The grid comprises three parts which are attached to each other: inlet with splitter plate, splitter plate wake region and pipe region. Grid points were concentrated near the trailing edge of the splitter plate in order to resolve the small scale mixing behaviour just downstream of the splitter plate, where the two fluid flows come in contact with each other. Use was made of the symmetry of the problem, and only the grid of half of the pipe was generated (Fig. 1).

The two fluids entered the computational domain with the same velocity and turbulence properties but with different temperatures $T_1 = 400$ K and $T_2 = 300$ K to simulate the different concentrations at the inlet. At the outlet the pressure was set constant across the entire outlet region, and the gradients for all other variables were held constant. Wall functions were applied to the wall boundaries at the pipe walls. In the wall function approach the near wall tangential velocity is related to the wall shear stress by means of a logarithmic relation.

Appropriate energy boundary conditions representing concentration boundary conditions had to be chosen. No fluid can leave or enter the domain through the wall of the pipe hence the suitable energy boundary condition is that of an adiabatic wall.

The character of the flow changes in the streamwise direction. Just downstream of the trailing edge of the splitter plate the flow is basically a free shear layer flow. With increasing thickness of the boundary layer the fluid flow becomes more and more a boundary layer type flow, especially when the boundary layer fills the whole pipe. From this follows that the turbulent Prandtl number in the case of heat transfer, or the turbulent Schmidt number if mass transfer is considered, changes from the value 0.5 for free shear layer flow to 0.9 for boundary layer flow. The turbulent Prandtl number depends significantly on the flow geometry (Cebeci and Bradshaw [10]). The program does not allow a change in the Prandtl number in the computational domain, hence a mean Prandtl number was used for the whole region. An estimation of the mean Prandtl number lead to a value of 0.6.

3.2. *Comparison with experimental data*

The results of the mixing process in the pipe are visualized in Fig. 1. The contours of equal temperature are shown in a cross section. The mixing process starts

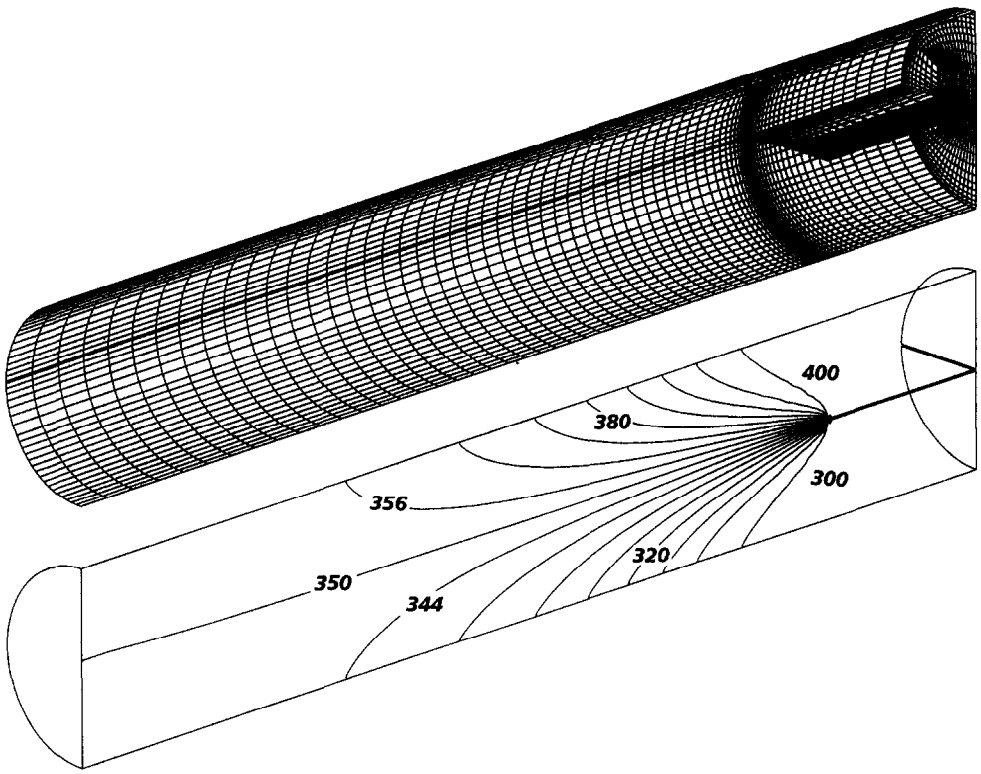

Fig. 1. Surface gridlines of the computational domain for the straight pipe problem and contours of equal temperature in a cross section.

at the trailing edge of the splitter plate, and this region extends in the downstream direction towards the pipe wall. The intensity of segregation was calculated along the pipe, and is shown in Fig. 2 together with the experimentally obtained data. The two curves show good agreement for two different Reynolds numbers. The good agreement of experimental and numerical data suggests that the TASCflow program is suitable to examine the complex mixing process in static mixers numerically.

4. THE FLUID FLOW AND THE MIXING PROCESS IN THE SMV MIXER

Static mixers are used to smooth out non-uniform distributions of fluid properties, like temperature or concentration with a minimum of pressure drop. The SMV mixer (see Fig. 3) is a device with a regular but rather complex structure designed to perform this task very efficiently.

To study the basic phenomena of the mixing process, the flow field in a section of the mixer which represents the typical flow behaviour and the mixing process of the whole mixer was calculated. Because of the regular and periodical structure of the SMV mixer the flow and the mixing process of that section is repeated periodically in the whole mixer. All the characteristic phenomena can be analysed in this subregion. The effects of the channel walls are not taken into account in the first analysis.

4.1. *Grid and boundary conditions*

The static mixer SMV consists of several corrugated blades. These corrugated sheets are stacked on each other. The folded edges of the sheets include a certain angle to the main flow direction. The angle is the same for all layers but adjacent layers are aligned in opposing directions.

The grid has been generated for a subregion which comprises the basic geometric structure of the SMV mixer. The grid comprises about 65 000 nodes. The number of grid nodes was kept as small as possible to obtain reasonable computing times.

To cover the whole domain of interest, static mixer and wake region, the domain was also split into three subdomains in the streamwise direction, and the calculations of the flow fields were carried out sequentially. A surface plot of the computational mesh is shown in Fig. 4.

The goal of the simulations was to investigate the mixing process in the SMV mixer. Thus the inlet region was divided into two parts. In both regions the inlet velocity was $v = 15\ \mathrm{m\ s^{-1}}$ and the density $\rho = 1.2$ kg $\mathrm{m^{-3}}$. The temperature for the upper half was $T = 301$ K and for the lower half $T = 300$ K. The turbulent properties were unknown and therefore had

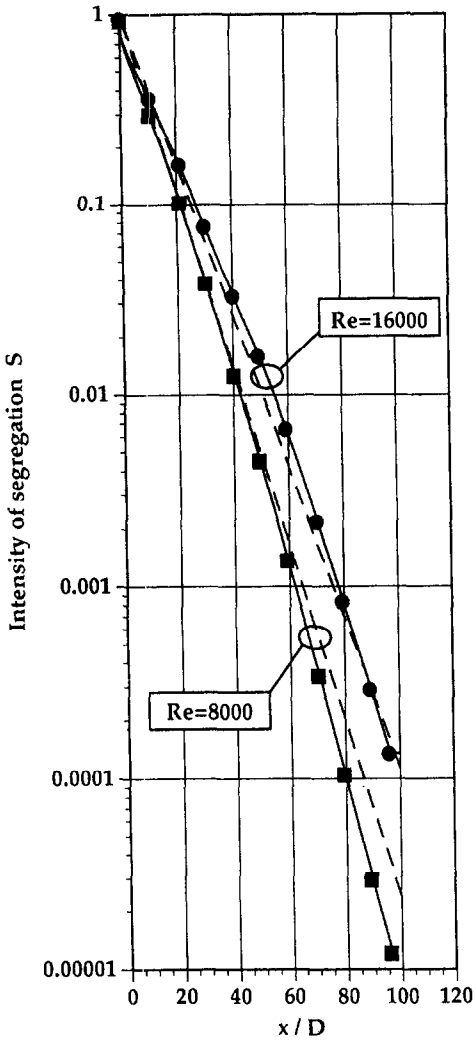

Fig. 2. Comparison of the computed and measured intensity of segregation along the pipe.

to be estimated. A reasonable guess is $I = 5\%$ for the turbulence intensity and $L_t = d_h/10$ for the turbulent length scale with a characteristic length of $d_h = 1.5$ m. The turbulence intensity was changed to $I = 1\%$ at the inlet to investigate the effect of turbulence inlet properties on the mixing process.

Periodic boundary conditions were applied to surfaces parallel to the main flow direction. This leads to a flow field which is infinite in the two directions perpendicular to the main flow direction. More precisely the flow pattern is repeated with the same geometric period of the subregion.

The simulations in the streamwise direction were performed sequentially. The distribution of the velocity components, the turbulence properties and the temperature profiles at the outlet became the inlet boundary conditions for the next section to be computed. It has been assumed that the downstream fluid flow does not influence the fluid upstream, or that the influence is negligible.

4.2. *Results*

The Reynolds number, based on the characteristic length and the main flow velocity, is $Re = 426\,000$. The mixing process is analysed by studying the velocity field and the temperature profiles in the SMV mixer and in the wake.

The velocity field gives a lot of information about the mixing process. The corrugated sheets divert the flow in the direction of their folded edges. This means that one sheet diverts the fluid to the right and the adjacent sheet to the left. In Fig. 5 the velocity components in the plane perpendicular to the main flow direction are shown. It can clearly be seen that the points, where two mixer sheets touch, are the starting points for vortices. The vortices which are generated by the first row of touching points in the main flow direction travel downstream till they disappear due to diffusion or are merged with the new vortices which are produced by the second and last row of touching points. These vortices can be found for a long distance downstream in the wake of the SMV mixer under ideal conditions (infinite size of mixer and no channel walls present), see Fig. 5.

The flow pattern described in the previous paragraph governs the mixing process. The mixing in a SMV mixer is mainly due to these vortices and not due to increased turbulent diffusion generated by the mixer structure. No significant difference in the mixing quality can be found if the turbulence intensity at the inlet is changed from $I = 5\%$ to $I = 1\%$. A considerable part of the mixing process occurs in the wake of the mixer.

A contour plot of the temperature in Fig. 6 for the cross section at the end of the mixer also shows the mixing behaviour induced by the structure of the mixer.

After about 10 characteristic lengths good mixing quality has been achieved.

The intensity of segregation was calculated for this mixing process, and is plotted as a function of the dimensionless mixer length in Fig. 7. The intensity of segregation decreases very rapidly in the downstream direction up to $y/d_h = 5$ where the mixing process seems to be quite intensive due to the arrays of vortices. The presence of channel walls slows the mixing process down as a computation showed. The vortices can still be found in the wake but they are not as regularly distributed as in the ideal case without walls. They are also distorted in shape. The diagram of the intensity of segregation clearly shows that the same mixing quality could not be achieved (Fig. 7). Both the ideal mixer and the mixer in a channel give much better results than the mixing process driven by turbulent diffusion alone as in the Hartung and Hiby [9] experiment (see Fig. 7).

5. INDUSTRIAL APPLICATION: THE MIXING PROCESS IN A DeNO$_x$ FACILITY

During the last decade the reduction of chemical compounds such as NO_x and SO_2 in flue gas emissions

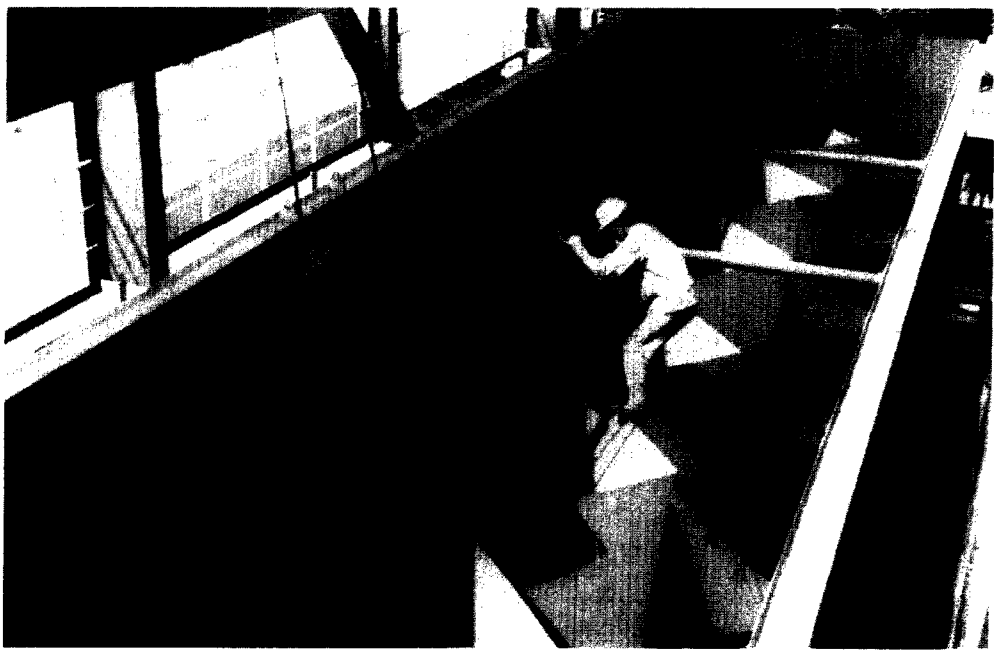

Fig. 3. SMV mixer for a $DeNO_X$ facility.

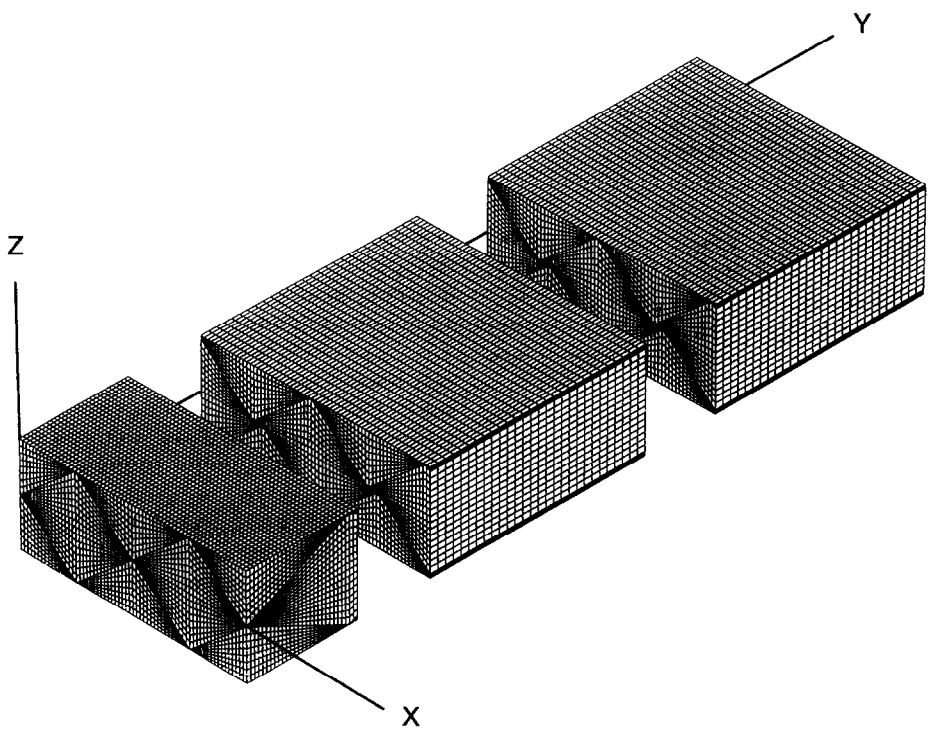

Fig. 4. Grid of the SMV mixer and the wake region.

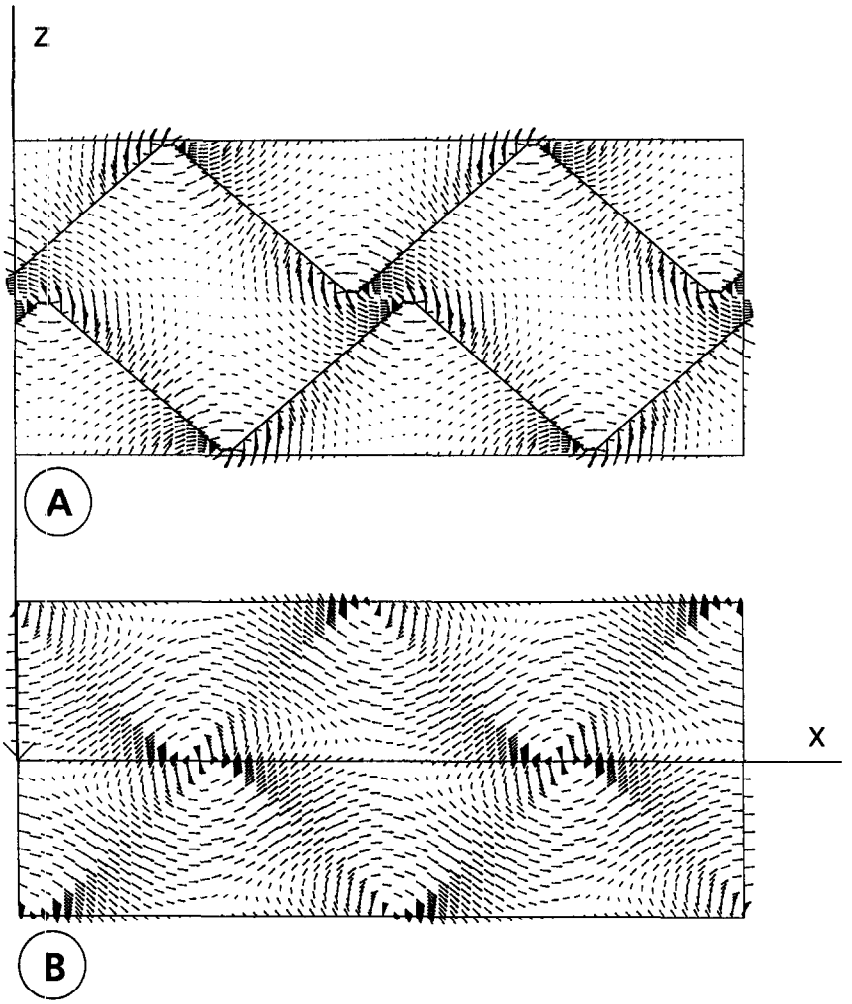

Fig. 5. Velocity vectors in a cross section within the mixer at $y = 0.538$ m (A) and in a cross section in the wake region at $y = 9.0$ m (B).

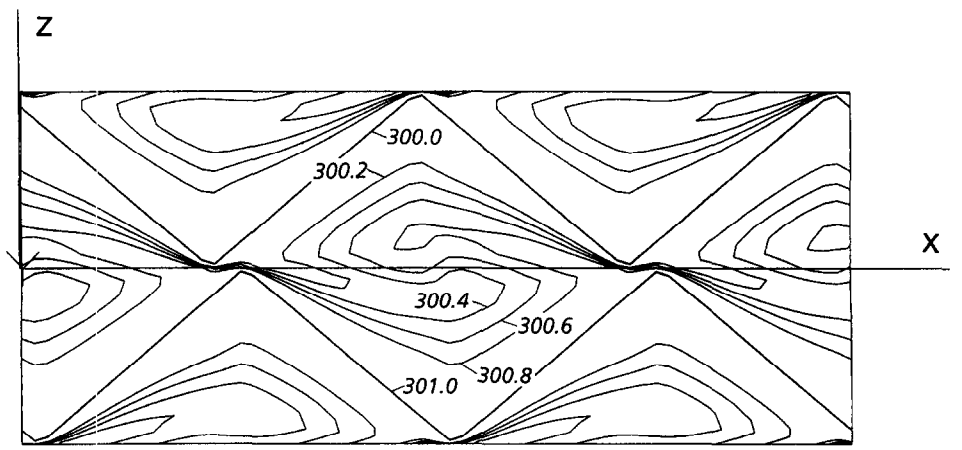

Fig. 6. Temperature distribution in the cross section at the end of the mixer at $y = 3.0$ m.

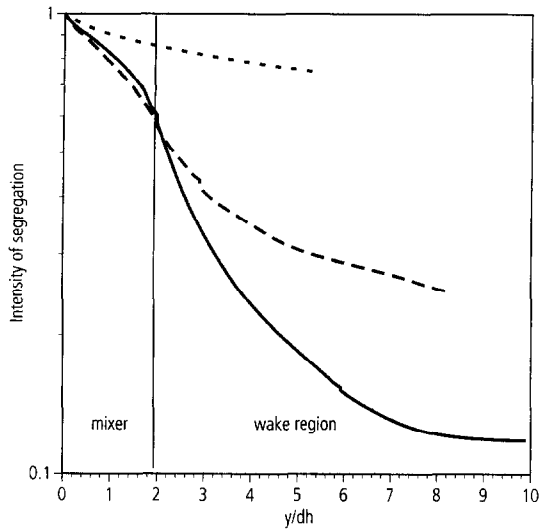

Fig. 7. The intensity of segregation plotted as a function of the dimensionless mixer length for pipe flow (----), ideal mixer (——) and mixer in channel (— — —).

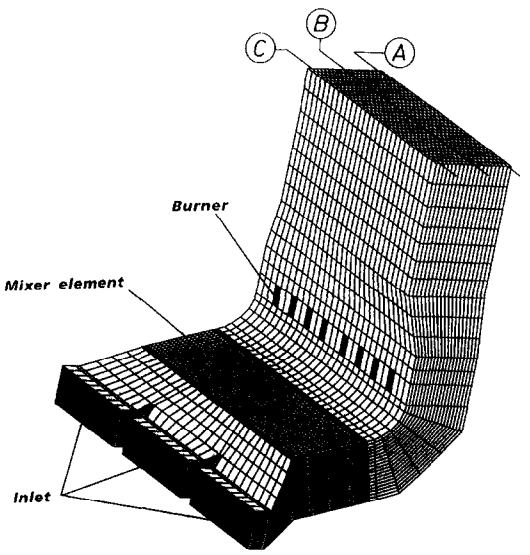

Fig. 8. Computational grid of the simulated part of the $DeNO_X$ facility. A, B and C denote lines where data has been compared.

from conventional power plants and waste incinerators has become more and more important due to stringent environmental protection regulations. Often the removal of nitrogen compounds is carried out by catalytic processes. The catalysts, which are usually arranged in several layers inside the reactor containment, require certain flow conditions. In particular the distributions for velocity, temperature and chemical species concentration in the flue gas stream have to fulfill strict tolerance criteria. The distribution of the flow variables should be as homogeneous as possible to get a uniform load and achieve optimal operating conditions. As a consequence, the flue gas flow has, in general, to be altered by appropriate means in order to satisfy all required conditions. This is usually achieved by employing static mixers, baffles and a number of guide vanes to improve the flow uniformity.

Here, numerical investigations are reported on the optimization of the fluid flow in a $DeNO_X$ facility inlet region. Experiments were carried out with a scale model (1 : 14), and with the same velocity as in reality. In the experiment the velocity and the concentration profiles were measured in certain planes perpendicular to the main flow direction. These data were compared to results of the numerical simulations of the fluid flow.

The calculation of the flow field and the concentration distribution in a whole $DeNO_X$ facility is not possible with our computer resources to date. We have therefore simulated only a part of the $DeNO_X$ facility. The section of the plant, which was calculated, comprises the triple inlet, the first mixer, the elbow and a channel section.

5.1. *Grid and boundary conditions*

The grid for this computation consists of three different parts. Part one comprises the section from the inlet to the SMV mixer, part two the SMV mixer and part three the channel section with elbow to a plane some distance downstream of the ammonia injection. The section which includes the mixer has a fine mesh to model the geometry of the mixer exactly, whereas the two other sections have coarse grids. While the grid of the SMV mixer consists of 89 375 gridpoints, the two other parts are modelled by 4200 and 12 000 nodes. This yields a total of 105 575 gridpoints. The grid for this computation can be found in Fig. 8. The generation of three different grids is possible because the program TASCflow allows two or more different grids to be attached to each other. This allows computations of complicated geometries because only the complex part must be modelled with high resolution. The SMV mixer used here has the dimensions: length $L_M = 3.4$ m, height $H_M = 3.0$ m and depth $B_M = 15.0$ m.

The mean flow velocity at the inlet was $v = 26.9$ m s^{-1}. The turbulence properties were chosen as follows: turbulence intensity $I = 5\%$ and turbulence length scale $L_t = 0.5$ m. To investigate the temperature equalization, the fluid temperature was set to $T_m = 400$ K in the middle section of the inlet, whereas the fluid temperature for the left and right section was set to $T_r = T_l = 300$ K. The channel walls were considered as adiabatic. The outlet boundary conditions prescribed were of constant static pressure across the outlet, and with the streamwise gradients of all variables taken to be zero.

5.2. *The mixing process*

The velocity distribution in planes perpendicular to the main flow direction is shown in Fig. 9. At the outlet of the computational domain near the plane where the ammonia is injected, strong velocity gradi-

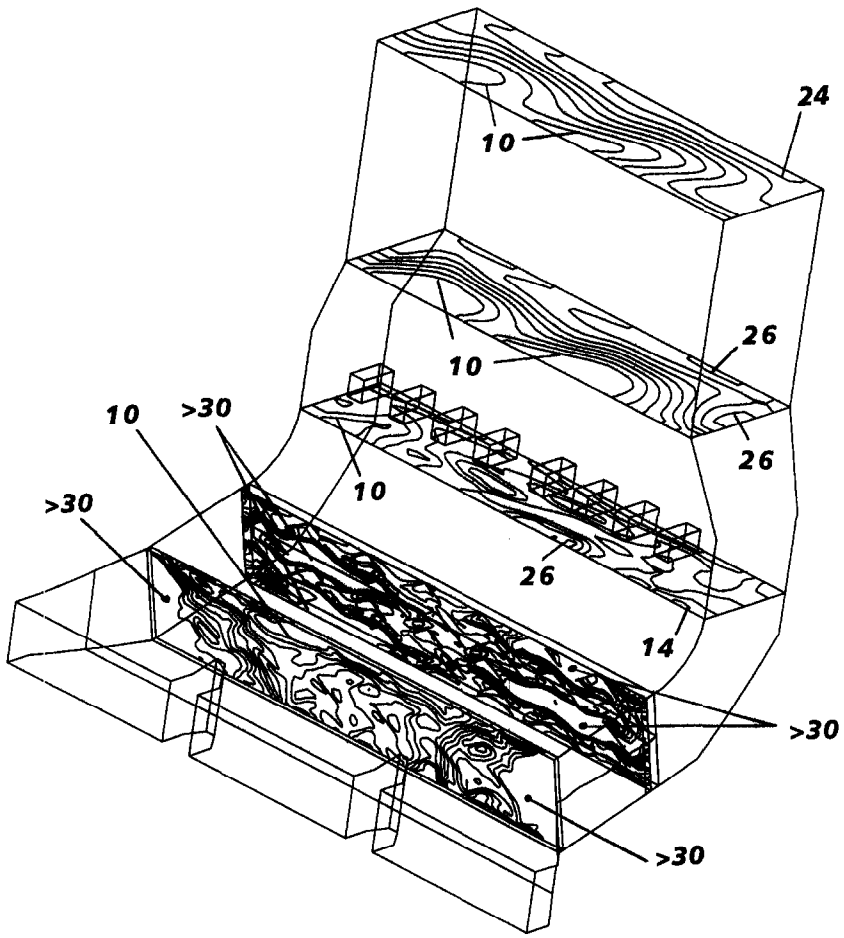

Fig. 9. Distribution of speed in planes perpendicular to the main flow direction. The numbers denote velocities in m s^{-1}.

ents can be found. These gradients are caused by two regions of low velocity. This is the result of the secondary flow in the bend and the burners which are located at the side of the low velocity regions. These burners are intended to be used when the temperature is too low, which occurs while the power plant operates at part load.

In Fig. 10 the temperature distribution in planes perpendicular to the main flow direction is shown. The mixing behaviour in the SMV mixer can easily be recognised. The hot flue gas which enters the facility through the middle inlet is diverted to left and right according to the orientation of the corrugated sheets. This can be observed in the first plane behind the mixer. In the wake of the mixer the flue gas is mixed due to the vortices which are generated as described in the previous chapter. This mixing process is supported by the secondary flow caused by the bend.

Computations have also been carried out without a static mixer and, as can be seen in Fig. 11, the temperature distribution in this case is rather different. The effect of the mixer is obvious. A much more uniform temperature distribution is achieved, and velocity differences are smoothed out.

5.3. *Comparison with measurements*

In the previous discussion results of the numerical simulations were analysed. The numerical results are of special interest because they provide an insight into the flow behaviour and the mixing process that is not possible to obtain by experiments. This information can provide hints where the flow patterns could be improved, and where the design should be changed.

As soon as numerical results and experimental data are available the question arises as to how accurate are the numerical results? In our case numerical and experimental data for velocity and temperature could be compared. The measured concentration and the calculated temperature as well as the measured and computed velocities are compared in the cross section some distance downstream of the ammonia injection. Details about the measurement technique used in the experiments can be found in Streiff *et al.* [11]. In Fig. 12 the measured concentration is compared with the

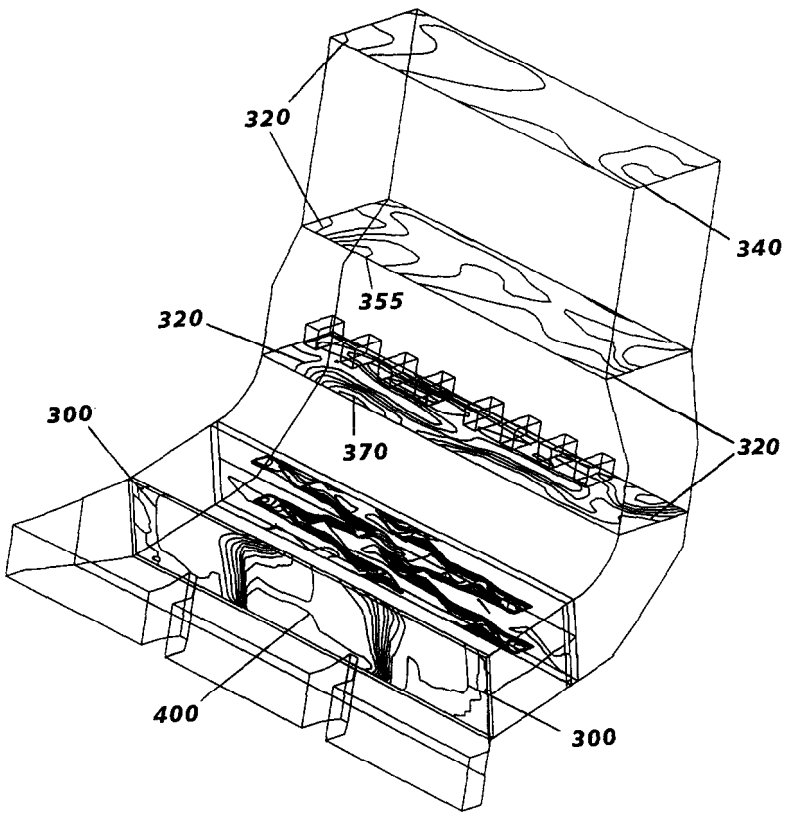

Fig. 10. Distribution of temperature in planes perpendicular to the main flow direction. The numbers denote temperature in kelvin.

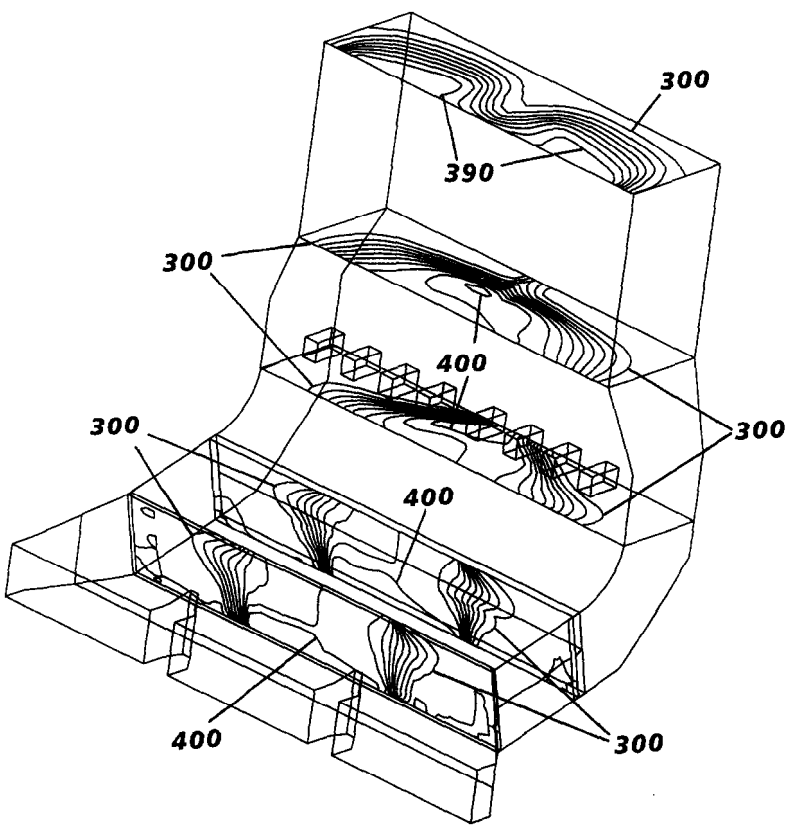

Fig. 11. Distribution of temperature in planes perpendicular to the main flow direction but without a static mixer. The numbers denote temperature in kelvin.

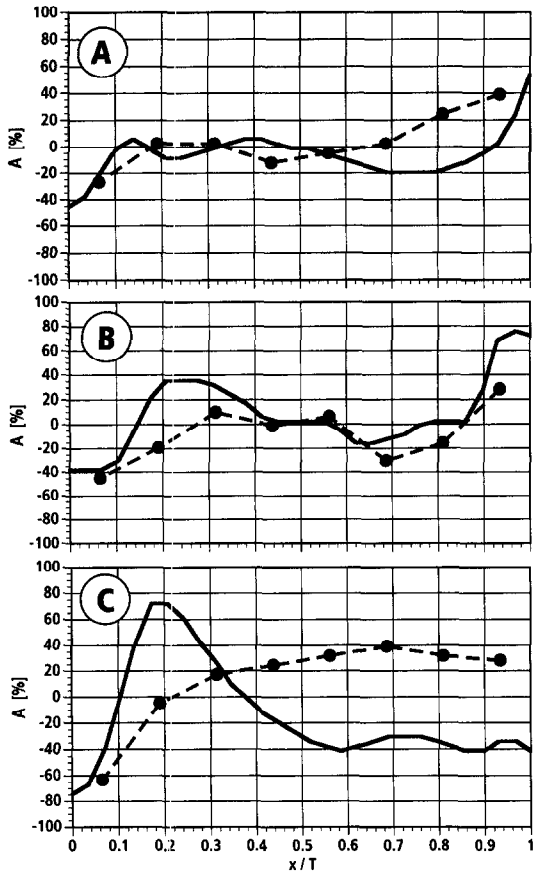

Fig. 12. Comparison of measured concentration and calculated temperature along the lines A, B and C as shown in Fig. 8.

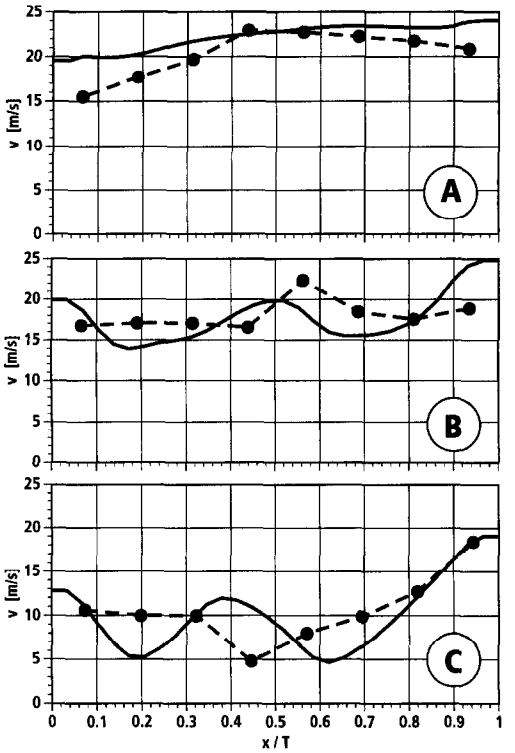

Fig. 13. Comparison of measured and computed speed along the lines A, B and C as shown in Fig. 8.

computed temperature along three lines. The position of the lines is given in Fig. 8. The deviation of the local to the mean value is calculated to be

$$A = \frac{T - \bar{T}}{\bar{T}} \tag{14}$$

for the temperature, and

$$A = \frac{c - \bar{c}}{\bar{c}} \tag{15}$$

for the species concentration. Good agreement is obtained near the wall opposite the burners. Just above the burners large differences can be found. This is caused by the rather coarse grid. A finer mesh resolution should lead to a much better agreement in this region. The measured and computed velocities are compared in Fig. 13, and good agreement is found.

6. SUMMARY AND CONCLUSIONS

The mixing process of the Hartung and Hiby experiment was analysed numerically. A comparison of measured data and numerical results for the intensity of segregation showed good agreement. This agreement suggests that numerical simulation can be used to compute fluid flows in static mixers.

The flow field in an idealised mixer without endwall effects was studied. The analysis showed that a considerable part of the mixing occurs in the wake of the SMV mixer. The mixer induces a set of vortices which are responsible for the mixing process. Turbulent diffusion is negligible.

As an industrial application the mixing process in part of a $DeNO_X$ facility was also investigated. The simulation showed that the temperature maldistribution was equalized by the mixing process initiated by the SMV mixer. Velocity differences were also smoothed out. The computed results were compared to experimental data, and good agreement was found.

The investigation showed that numerical simulations can be used to compute the fluid flow and the mixing process in static mixers. A numerical simulation can give much more insight into the flow and the mixing of such a facility because the simulation gives data at every gridpoint, whereas the experiment only gives data at locations where measurements have been carried out. This can lead to a better design and a faster design process. This in turn leads to facilities with higher efficiencies, and reduced operating costs.

Acknowledgement—This work was partly supported by Noell-KRC Umwelttechnik Ltd.

REFERENCES

1. J. C. Godfrey, Static mixer. In *Mixing in the Process Industries* (Edited by N. Harnby and A. W. Nienow), Chap. 13. Butterworth Series in Chemical Engineering, London (1985).
2. W. Tauscher, F. Streiff and R. Bürgi, Statisches Mischen von Gasströmen in großen Leitungen, *VGB Kraftwerkstechnik* **60** (1980).
3. M. Zogg, Strömungs- und Stoffaustauschuntersuchungen an der Sulzer-Gewebepackung, Dissertation 4886, ETH Zürich (1972).
4. G. Gaiser, Strömungs- und Transportvorgänge in gewellten Strukturen, Dissertation, Universität Stuttgart (1990).
5. P. Drtina, E. Lang, M. Fleischli and F. Streiff, Optimization of a $DeNO_X$ facility by numerical simulation, *Proceedings of UIT XI Congresso Nazionale sulla Trasmissione del Calore*, Milano (1993).
6. Bird, Stewart and Lightfoot, *Transport Phenomena*. Wiley, New York (1960).
7. B. E. Launder and D. B. Spalding, The numerical computation of turbulent flows, *Comp. Meth. Appl. Mech. Engng* **3**, 269–289 (1974).
8. TASCFlow User Manual, Advanced Scientific Computing Ltd, Waterloo, Canada (1993).
9. K. H. Hartung and J. W. Hiby, Beschleunigung der turbulenten Mischung in Rohren, *Chem. Ing. Tech.* **44**, 1051–1056 (1972).
10. T. Cebeci and P. Bradshaw, *Physical and Computational Aspects of Convective Heat Transfer*. Springer, Berlin (1988).
11. F. Streiff, M. Fleischli, P. Drtina and E. Lang, Optimierung von Entstickungsreaktoren durch statische Mischsysteme und numerische Strömungsberechnungen, VGB Kraftwerkstechnik **73**, 450–455 (1993).